

Analysis of Wideband Radio Channel Properties for Planning of Next-Generation Wireless Networks

Haibin Zhang^{#1}, Onno Mantel^{#2}, Maurice Kwakkernaat^{*3}, Matti Herben^{*4}

[#]*TNO Information and Communication Technology
P.O.Box 5050, 2600 GB Delft, The Netherlands*

¹haibin.zhang@tno.nl

²onno.mantel@tno.nl

^{*}*The Eindhoven University of Technology
5600 MB Eindhoven, The Netherlands*

³maurice.kwakkernaat@ieee.org

⁴m.h.a.j.herben@tue.nl

Abstract—This paper analyzes the application of wideband channel properties in the radio planning of wideband wireless networks. The definition and prediction of delay spread (DS) and angular spread (AS) are first discussed. A wideband high-resolution measurement campaign is then described which was conducted in an urban area using a 3-D high-resolution channel sounder. The comparison between measured and predicted data shows different prediction accuracy of DS and AS, with a 3-D ray tracing approach, for two different propagation environments.

I. INTRODUCTION

In current radio planning of mobile networks, the system performance analysis is based on signal-to-noise ratio (SNR) requirements for specific data or reference channels in the system, with the assumption of narrow-band communication. The continuous demand for increased throughput currently drives the world-wide deployment of wireless wideband communication systems, such as WiMAX and Long-Term Evolution (LTE). In these systems, orthogonal frequency-division multiplexing (OFDM) and multiple-input multiple-output (MIMO) technologies are used. For MIMO-OFDM-based systems, the system performance depends not only on the SNR, but also on the amount of frequency and spatial diversity the system can exploit [1] [2]. For a specific reference channel (and thus a specific combination of modulation, coding and signal format), these diversities rely on the delay and angular profiles of the radio channel, which are often quantified in terms of delay spread (DS) and angular spread (AS), respectively [3] [4]. The performance of future mobile networks will thus depend not only on the SNR, but also on these wideband radio channel properties. For an effective radio planning of these networks, these properties should be taken into account. Predictions of the angular and delay profiles of the channel can be made with propagation models based on ray-tracing [5] [6]. The accuracy of these predictions will determine their potential for use in the planning of wireless wideband networks.

In this paper, we analyse the use of wideband radio channel properties in the radio planning of MIMO-OFDM-based wireless systems. To this end, we compare the predictions of an off-the-shelf ray-tracing model with the results of high-

resolution channel sounding measurements. The compared channel parameters are the received power, the delay spread, and the azimuth angular spread at the mobile station (MS) side.

The paper is organized as follows. Section II gives definitions of the delay spread and angular spread. Section III describes how predictions of these parameters are made. The measurement set-up and the test scenario are described in Section IV. The numerical evaluation of the comparison is presented in Section V. The paper ends with a conclusion.

II. DEFINITION OF DELAY AND ANGULAR SPREAD

In our investigation, we focus on the DS and azimuth AS at the MS side. In principle, the AS at the base station (BS) side might also affect the performance of MIMO systems. However, for an urban area with roof-top BS antennas, the AS and its absolute variation at the BS side are much smaller than those of the AS at the MS side [1]. We also do not consider the elevation AS at this stage, since it is generally much smaller than the azimuth AS [7] and it is not made available by the ray-tracing prediction tool we used.

The delay spread T_σ is here defined as the standard deviation of the delay values of reflections, weighted proportional to the power in the reflected waves, i.e.,

$$T_\sigma = \sqrt{\frac{\sum_n (t_n - \bar{T})^2 \cdot P_n}{\sum_n P_n}} \quad (1)$$
$$\bar{T} = \frac{\sum_n t_n \cdot P_n}{\sum_n P_n}$$

where \bar{T} is the power-weighted mean delay, and t_n and P_n are the delay and power of path n respectively. Chuang [3] showed that the shape of delay profile has little effect on radio performance, whilst the delay spread has significant effect. For OFDM systems, as long as the maximum delay does not exceed the guard interval, the longer delay spread introduces higher frequency diversity with the assistance of frequency-domain interleaving and channel coding. Schenk *et al.* [8]

showed an about 5 dB performance gain of $T_\sigma = 100$ ns over $T_\sigma = 30$ ns at packet error rate of 10^{-2} , for an OFDM-based IEEE 802.11a system configured with 3x3 MIMO.

AS can be used as an important parameter of spatial channel model for MIMO simulations [1] [4]. However, the definition of angular spread θ_σ is not as simple as that of delay spread, since angle is a type of circular data. Here, we compare the following three definitions of AS, given by Fisher [9], Fleury [10], and Winprop (the tool we used for prediction, see Section III) respectively.

- Definition Fisher:

The AS is defined as the *circular standard deviation*:

$$\theta_\sigma = \sqrt{-2 \log(R)} \quad (2)$$

$$R = \left| \sum_n \exp(j\theta_n) \cdot P_n \right| / \sum_n P_n$$

where θ_n is the azimuth angle of arrival of path n .

- Definition Fleury:

The AS is defined as the square root of the *circular variance* $V = 1 - R$:

$$\theta_\sigma = \sqrt{V} = \sqrt{1 - R} \quad (3)$$

$$R = \left| \sum_n \exp(j\theta_n) \cdot P_n \right| / \sum_n P_n$$

- Definition Winprop:

The AS is defined as follows:

$$\theta_\sigma = \sqrt{\frac{\sum_n (\theta_n - \bar{\theta})^2 \cdot P_n}{\sum_n P_n}} \quad (4)$$

$$\bar{\theta} = \angle R = \angle \left[\sum_n \exp(j\theta_n) \cdot P_n \right] / \sum_n P_n$$

where “ $\angle(\cdot)$ ” denotes the angle.

Note that the definitions of Fisher and Fleury are quite similar in physical principle. The only difference is whether the angular spread is defined as the circular standard deviation, or as the square root of the circular variance. For circular variables, the circular standard deviation is not necessarily the same as the square root of the circular variance [9].

Fig. 1 shows the azimuth angular spread (at the MS side) of Site 1 in our measurement campaign (see Section IV) calculated using the three definitions, respectively. The angular spread is averaged per 10×10 m² prediction pixel (see Section V), to exclude noise. The values are scaled so that ASs calculated using different definitions have the same maximum value, for the sake of comparison. It's shown that, although a bit different in concrete values, the ASs calculated using different definitions have almost the same trends of change. Thus no significant effect on wideband planning is expected by using different definitions of AS. In our further investigation, we will use the definition used by Winprop.

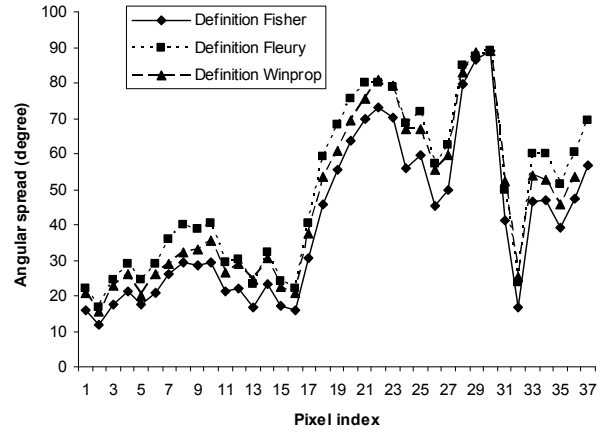


Fig. 1 Comparison of angular spreads calculated using different definitions

III. PREDICTION OF DELAY AND ANGULAR SPREAD

For the prediction of delay spread and angular spread we use the software package WinProp, version 8.15, offered by AWE Communications [11]. With this package, the radio channel can be modelled using ray-tracing techniques.

In ray-tracing, the propagation of the radio signal is approximated by constructing rays that travel between transmitter and receiver. Each ray interacts with objects in the environment, by means of reflection, diffraction, or scattering. The signal at the receiver is obtained by combining the different ray paths that arrive from different angles and at different arrival times.

Ray-tracing techniques can provide an accurate modelling of propagation behaviour in complex outdoor environments such as dense urban areas. However, the involved computation times can be quite prohibitive when evaluating a larger-scale urban scenario such as typically encountered in mobile network planning. This is mainly due to the computational effort required to derive the possible ray trajectories from the building configuration.

In WinProp, computation time is reduced by introducing an off-line preprocessing step [5]. During the preprocessing, visibility relations between building wall tiles are derived and stored in a separate building database file. When making predictions, the visibility information is used to quickly construct the ray paths.

For the predictions described in this paper, preprocessing of the building data has been performed using the default wall tile size and wedge segment size of 100 meters. Typical computation times of prediction are then of the order of 20 minutes for the scenarios studied in this paper, using a regular Windows machine.

The propagation model selected in WinProp is 3D intelligent ray-tracing. Reflections and diffractions are modelled by user-defined empirical loss values. No transmission through buildings is considered. The number of interactions per ray is limited to two reflections and one diffraction; rays with more interactions are ignored. The amount of rays is further limited by imposing a maximum

path loss of 200 dB per ray, a maximum dynamic range of 35 dB for the ray contributions in one pixel, and a maximum path number of 50.

The decay of signal level with distance is described by a path loss exponent, which can be tuned for optimal performance. Different path loss exponents can be set for line-of-sight (LOS) and non line-of-sight (NLOS) conditions. In this study we have used the default setting, which means a path loss exponent of 2.6 for both LOS and NLOS conditions.

All predictions are made for the center of each $10 \times 10 \text{ m}^2$ pixel within a $1200 \times 1200 \text{ m}^2$ area. The delay spread and azimuth angular spread are generated per pixel, according to the Winprop definition described in Section II.

IV. HIGH-RESOLUTION MEASUREMENT CAMPAIGN

The measurement data used in this paper is obtained using a recently developed 3-D high-resolution channel sounder [12]. The system is based on a 3-D tilted-cross switched antenna array that consists of 31 monopole antennas and uses an improved version of the 3-D Unitary ESPRIT algorithm to obtain signal parameter estimates at mobile conditions. The measurement system operates at a centre frequency of 2.25 GHz in a band of 100 MHz and is able to produce complex impulse responses with a range of $5.1 \mu\text{s}$ in the delay domain and a dynamic range of 35 dB. The resolution in the delay domain is 20 ns and samples are available at 10 ns instances. Using multiple snapshots, high-resolution angle-of-arrival (AOA) estimates can be obtained under mobile conditions at each delay instant in both azimuth and elevation with a typical resolution better than 5 degrees and an accuracy of 0.1 degrees. A single measurement snapshot is taken every $6.5 \mu\text{s}$ and sets of 10 consecutive snapshots are used as input for the 3-D Unitary ESPRIT algorithm. As a result, the angle and delay characteristics of the channel are estimated every $65 \mu\text{s}$.

Two independent measurements were performed in which the transmitter was placed at both BS locations: Site 1 and Site 2 as shown in Fig. 2. The transmitting antenna consisted of an 8-dBi waveguide horn antenna with an azimuthal half-power-beam-width of 55 degrees. A tripod is used to elevate the antenna such that it is in almost the same position and has the same orientation as the original BS antennas. The antenna tilt is 0 degree, and the antenna directions of Site 1 and Site 2 are 300 degree and 70 degree respectively. The transmit power is 43 dBm.

In the first experiment the transmitting antenna was positioned at Site 1, outside, at a height of 29 m above ground level. The scenario consists of both LOS and NLOS, which is caused by the temporary obstruction due to two large buildings along the trajectory (HvA1 and HvA2 in Fig. 2). In the second experiment the transmitting antenna was positioned at Site 2, outside, at a height of 27 m above ground level. This scenario is NLOS and propagation takes mainly place via reflections, surface scattering and through-building propagation.

The receiving antenna, mounted on top of a vehicle at a height of 3.5 m, was moved at a nearly constant speed of about 27 km/h over a trajectory of approximately 400 m for

both the first and second experiments. The exact measurement routes are slightly different by several meters, which results in a few different pixels for the prediction. A total of 9900 snapshot-sets of 10 snapshots are used for the AOA estimation, which means that a channel estimate is available every 4.5 cm, corresponding to 0.34 wavelengths. The first part of the measurement (approximately 6 prediction pixels) is affected by a railway crossing, which is not included in the building database for prediction and might contribute significantly to rough surface scattering.

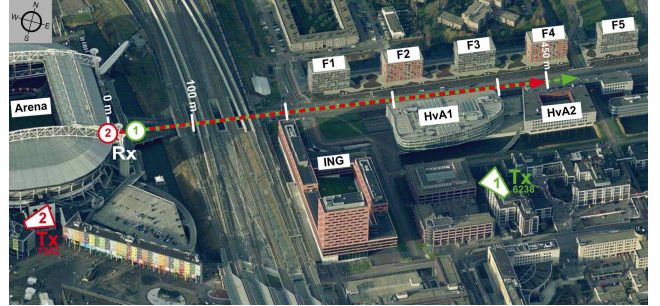


Fig. 2 Layout of the measurement site. The green and red lines represent the measurement trajectories with the transmitter active at Site 1 and Site 2, respectively. The map is from Microsoft Virtual Earth.

V. NUMERICAL EVALUATION

The measurement routes coincide with 37 prediction pixels for Site 1 and 36 prediction pixels for Site 2. Since the predictions are made *per pixel*, for the sake of comparison, the measured data are averaged and mapped to prediction pixels in the following procedure:

- First, each measurement snapshot is mapped to the pixel, whose centre is closest to the location where the measurement snapshot is recorded;
- Second, the received power, DS and AS values of all snapshots that were mapped to the same pixel are averaged to provide one measured value per pixel.

A. Prediction accuracy of received power

Fig. 3 shows plots of the measured and predicted received power, for Site 1 and Site 2 respectively. Table I shows the mean and standard deviation of the prediction error, which is defined as the difference between predicted and measured received power. The first 6 pixels are excluded in the calculation of the prediction accuracy, since they are affected by the railway crossing (also for the statistical calculation of DS and AS in the following sub-sections).

TABLE I
PREDICTION ERROR OF RECEIVED POWER

	Mean (dB)	Standard deviation (dB)
Site 1	0.7	4.4
Site 2	0.8	4.8

For both Site 1 and Site 2, a standard deviation of less than 5 dB is observed, which is generally considered as good prediction accuracy. For Site 1, the two peaks caused by LOS conditions are well predicted. For Site 2, no LOS conditions occur, in agreement with the measurements. At the beginning

of the measurement route the predictions are over-estimated for both Site 1 and Site 2. This can partly be due to the missing of the railway crossing in the building database.

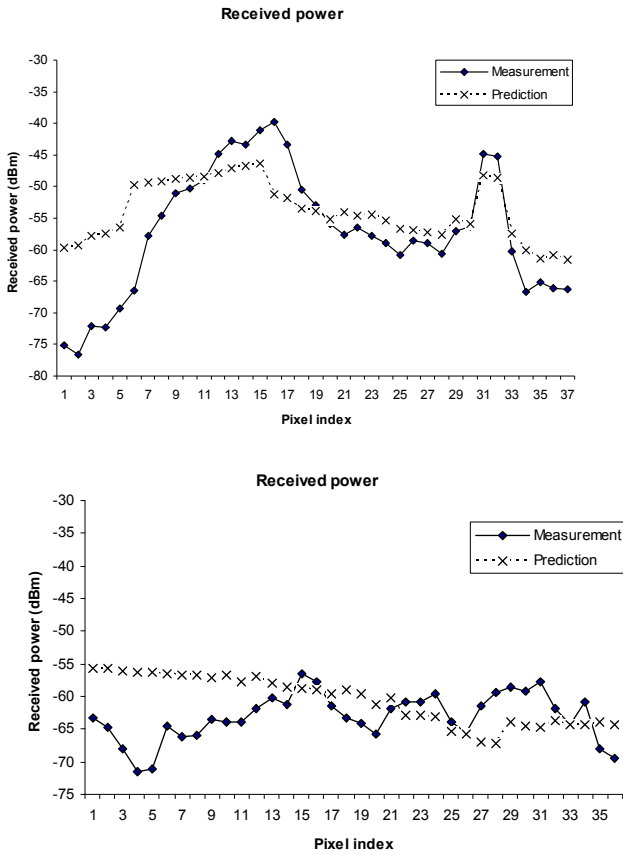


Fig. 3 Measured and predicted received power: Site 1 (top); Site 2 (down).

B. Prediction accuracy of DS

Fig. 4 shows plots of the measured and predicted DS, for Site 1 and Site 2 respectively. Table II shows the mean and standard deviation of absolute and relative prediction error of the DS. The values of absolute error are obtained by subtracting measurement values from prediction values per pixel. The relative values are obtained by dividing this absolute error by the measurement value per pixel. A relative error smaller than 0 means under-estimation, while a relative error larger than 0 means over-estimation. The relative value should be considered more important if one assumes that the inaccuracy of delay spread predictions scales with the delay-spread value itself.

For Site 1, the DS is overestimated in the first 5 pixels. This may be due to some effect from the railway crossing. For the other pixels, the predicted values are in most cases quite close to the measured values. However, for some of the other pixels (e.g. pixel 27) a large prediction error is observed. The cause of this has not yet been further investigated.

For Site 2, the prediction accuracy is worse than for Site 1. One reason might be the effect of the railway crossing, which is geographically between Site 2 and the measurement routes and thus might have more effect on Site 2 than on Site 1.

One of the parameters that can influence the accuracy of the DS predictions is the wall tile size used during preprocessing. For the current results, this size has been set to the relatively large default value of 100 m. By lowering the tile size, the more detailed visibility relations are obtained during the database preprocessing. This could further improve the prediction accuracy.

The results for the DS are roughly comparable to the results reported in [5], which were obtained for an urban scenario in Helsinki.

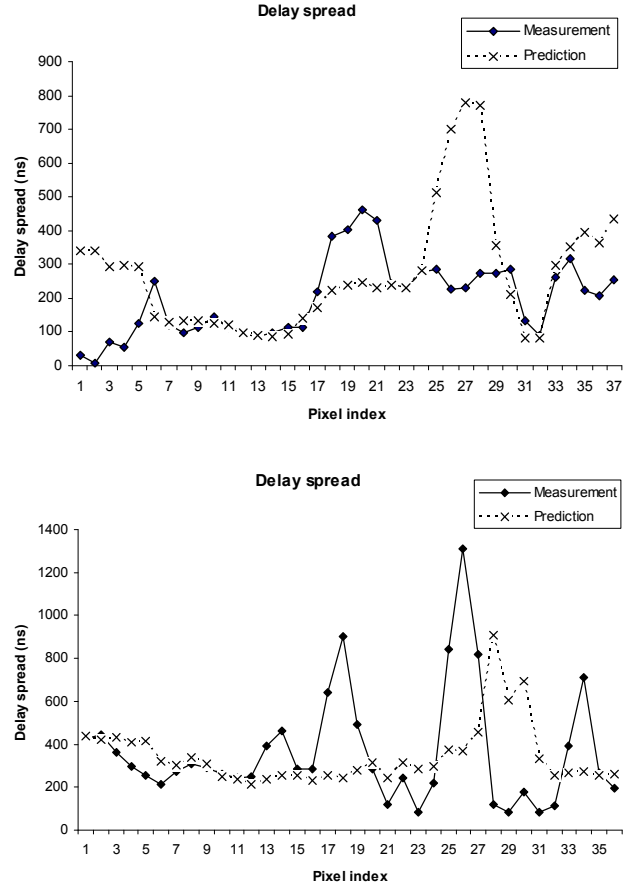


Fig. 4 Measured and predicted delay spread: Site 1 (top); Site 2 (down).

TABLE II
PREDICTION ERROR OF DELAY SPREAD

	Mean	Standard deviation
Site 1 (absolute)	49 ns	181 ns
Site 2 (absolute)	-41 ns	343 ns
Site 1 (relative)	0.24	0.71
Site 2 (relative)	0.64	1.9

C. Prediction accuracy of AS

Fig. 5 shows plots of the measured and predicted AS, for Site 1 and Site 2 respectively. Table III shows the mean and standard deviation of absolute and relative prediction error of the AS. Definitions of these statistical values are analogous to the definition for DS.

For Site 1, the over-estimation in the first five pixels can be explained from the effect of the railway crossing. For most other pixels, the predicted values are quite close to the measured values. However, for some pixels (e.g. pixel 16) a large prediction error is also observed. The cause of this has not yet been further investigated.

For Site 2, the prediction accuracy is similar to Site 1. In the part of the route between pixel 8 and 20, the measured angular spread is significantly larger than the prediction. This may be explained from the missing of building surface scattering in the predictions.

Just as for the DS, the accuracy of AS may be improved by decreasing the wall tile size used during preprocessing of the building data.

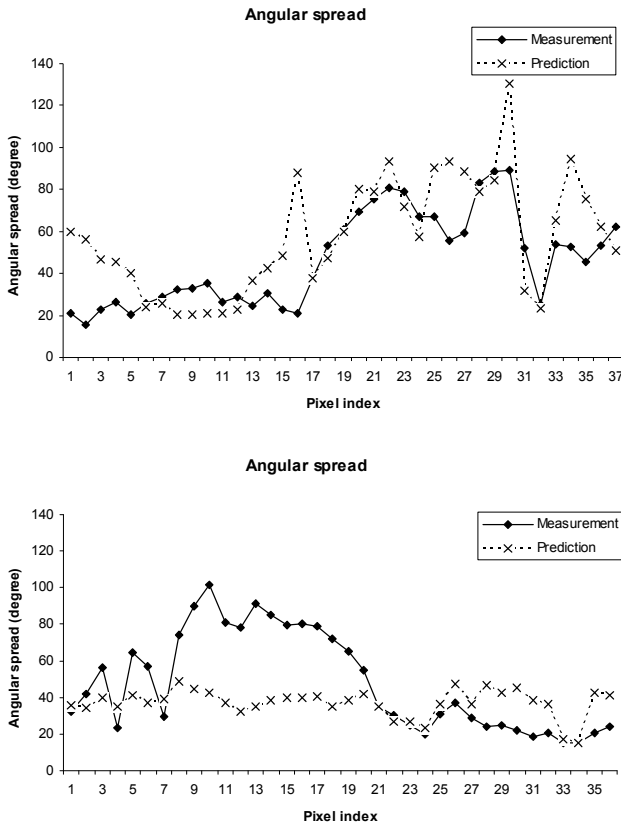


Fig. 5 Measured and predicted angular spread: Site 1 (top); Site 2 (down).

TABLE III
PREDICTION ERROR OF ANGULAR SPREAD

	Mean	Standard deviation
Site 1 (absolute)	7.6 degree	20 degree
Site 2 (absolute)	-11 degree	27 degree
Site 1 (relative)	0.20	0.67
Site 2 (relative)	0.04	0.57

VI. CONCLUSIONS

In this paper we have presented a comparison of wideband radio channel parameters predicted with a ray-tracing tool with the results of high-resolution measurements. The

comparison has been done for two test sites in a dense urban environment.

The numerical evaluation shows good prediction accuracy of the received power for both sites (with standard deviations less than 5 dB), which have quite different propagation conditions. This illustrates the relative robustness of predicting received power with 3D ray-tracing techniques.

On the other hand, the prediction accuracy of delay and angular spread varies significantly along the measurement route. This indicates that the accuracy of predicted wideband parameters is less robust towards limitations in the modeling of the environment. In our investigation, this limitation might be partly caused by surface irregularities.

As a follow-up, we intend to perform more measurements in other outdoor locations in urban areas. Also the effect of different ray-tracing parameters on the prediction accuracy should be further studied.

ACKNOWLEDGMENTS

The work in this paper has been financially supported by KPN. The authors would like to thank their colleagues Job Oostveen, Yohan Toh and Rainier van Dommele for their cooperation. AWE Communications, and in particular Oliver Stabler, is acknowledged for kind technical support in using Winprop and for fruitful discussions.

REFERENCES

- [1] 3GPP Document TR 25.996, "Spatial channel model for MIMO simulation (release 7)".
- [2] 3GPP Document TS 36.104, "E-UTRAN: Base Station (BS) radio transmission and reception.
- [3] J.C.-I. Chuang, "The effects of time delay spread on portable radio communications channels with digital modulation", *IEEE journal on selected areas in communications*, SAC-5(5), Jun. 1987.
- [4] A. van Zelst, J. Hammerschmidt, "A single coefficient spatial correlation model for multiple input multiple output (MIMO) radio channels", [online]. Available: <http://www.brabantbreedband.nl/PDF/Publications/Zelst%20coefficient%20URSI%2002.pdf>.
- [5] T. Rautiainen, G. Wölfle, and R. Hoppe, "Verifying path loss and delay spread predictions of a 3D ray tracing propagation model in urban environment", *Proc. IEEE Vehicular Technology Conference 2002-Fall*. Page(s): 2470 - 2474, vol.4.
- [6] J. Rossi, Y. Gabillet, "A mixed ray launching/tracing method for full 3-D UHF propagation modelling and comparison with wide-band measurements", *IEEE Trans. on Antennas and Propagation*, vol. 50, no. 4, Apr. 2002.
- [7] H. M. El-Sallabi, P. Vainikainen, "Impacts of environment and antenna height on angular spread of radio wave propagation in a city street microcell", *Proc. IEEE International Symposium on Antennas and Propagation*, 2000, pp:1146 - 1149 vol.2
- [8] T. C. W. Schenk, G. Dolmans, and I. Modonesi, "Throughput of a MIMO OFDM based WLAN", *Proc. SCVT'2004*, Nov. 2004.
- [9] N. I. Fisher, *Statistical Analysis of Circular Data*, Cambridge, UK: Cambridge University Press, 1993.
- [10] B. H. Fleury, "First- and second-order characterization of direction dispersion and space selectivity in the radio channel", *IEEE Trans. on Information Theory*, vol. 46, no. 6, pp. 2027-2044, Sept. 2000.
- [11] <http://www.awe-communications.com/>.
- [12] M.R.J.A.E. Kwakkernaat, Y.L.C. de Jong, R.J.C. Bultitude, and M.H.A.J. Herben, "High-resolution angle-of-arrival measurements on physically-nonstationary mobile radio channels," *IEEE Trans. Antennas and Propagation.*, vol. 56, no. 8, pp. 2720-2729, Aug. 2008.